Inorganic Chemistry

Article

pubs.acs.org/IC

# Formation of Hexagonal Fullerene Layers from Neutral and Negatively Charged Fullerenes in $\{(Ph_3P)_3Au^+\}_2(C_{60}^{\bullet-})_2(C_{60})\cdot C_6H_4Cl_2$ Containing Gold Cations with the $C_{3v}$ Symmetry

Dmitri V. Konarev,*[,†] Salavat S. Khasanov,[‡] Akihiro Otsuka,[§] Manabu Ishikawa,[§] Hideki Yamochi,[§] Gunzi Saito,[∥] and Rimma N. Lyubovskaya[†]

[†]Institute of Problems of Chemical Physics RAS, Chernogolovka, 142432, Russia

[‡]Institute of Solid State Physics RAS, Chernogolovka, Moscow region, 142432, Russia

[§]Research Center for Low Temperature and Materials Sciences, Kyoto University, Kyoto 606-8501, Japan

[∥]Faculty of Agriculture, Meijo University, 1-501 Shiogamaguchi, Tempaku-ku, Nagoya 468-8502, Japan

Supporting Information

**ABSTRACT:** Fullerene salt $\{(Ph_3P)_3Au^+\}_2(C_{60}^{\bullet-})_2(C_{60})\cdot C_6H_4Cl_2$ (**1**) containing $(Ph_3P)_3Au^+$ cations with the $C_{3v}$ symmetry has been obtained as single crystals. Hexagonal corrugated fullerene layers formed in **1** alternate with the layers consisting of $(Ph_3P)_3Au^+$ and $C_6H_4Cl_2$ along the *c* axis. According to IR spectra and peculiarities of the crystal structure, the charge on fullerenes in the layers is evaluated to be −1 for two and close to zero for one $C_{60}$. These fullerenes have different cationic surroundings, and positively charged gold atoms approach closer to $C_{60}^{\bullet-}$. Charged and neutral fullerenes are closely packed within hexagonal layers with an interfullerene center-to-center distance of 10.02 Å and multiple short van der Waals C···C contacts. The distances between $C_{60}^{\bullet-}$ are essentially longer with an interfullerene center-to-center distance of 10.37 Å due to corrugation of the layers, and no van der Waals contacts are formed in this case. As a result, each $C_{60}^{\bullet-}$ has only three negatively charged fullerene neighbors with rather long interfullerene distances providing only weak antiferromagnetic interaction of spins in the fullerene layers with a Weiss temperature of −5 K.

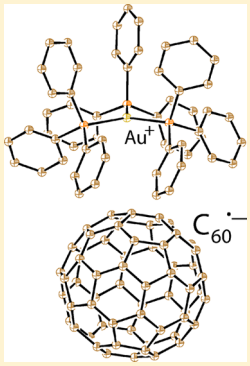


## INTRODUCTION

Ionic fullerene complexes can show promising magnetic and conducting properties.[1,2] Such properties are observed when closely packed fullerene radical anions provide magnetic interactions of spins[1] or movement of electrons[2] but are not dimerized since dimeric phases are diamagnetic and nonconducting.[3] The cationic sublattice plays a key role in the development of highly conducting fullerene packing since it defines the fullerene radical anions packing motif. For example, in TDAE·$C_{60}$ (TDAE: tetrakis(dimethylamino)ethylene), linear close packing of $C_{60}^{\bullet-}$ is formed, and mutual orientation of fullerene anions governs the ferromagnetic or antiferromagnetic interaction of spins.[1] The closely packed hexagonal fullerene layers in the $(MDABCO^+)(C_{60}^{\bullet-})(TPC)$ complex (MDABCO$^+$ is N-methyldiazabicyclooctanium cation; TPC is triptycene) allowed the quasi-two-dimensional metallic conductivity stable down to 1.9 K.[2d] Several highly conducting or even metallic compounds have closely packed hexagonal fullerene layers, for some of which the supposed crystal structures were based on unit cell parameters.[2] However, even a slight increase in interfullerene distances in the hexagonal fullerene layers, for example, in the $(MQ^+)(C_{60}^{\bullet-})(TPC)$ complex (MQ$^+$: *N*-methylquinucledinium cation), provides the Mott insulator with an antiferromagnetic spin-frustrated ground state.[4] Thus, namely, closely packed hexagonal fullerene layers in the absence of dimerization can provide high conductivity.[2e]

To obtain such layered systems, the cations or neutral components with the $C_{3v}$ symmetry can be used to arrange fullerene anions in a hexagonal manner. Both MDABCO$^+$ cations and neutral TPC molecules have the $C_{3v}$ symmetry in $(MDABCO^+)(C_{60}^{\bullet-})(TPC)$, resulting in the formation of hexagonal fullerene layers.[2d] In this work, we used gold $(Ph_3P)_3Au^+$ cations, whose symmetry is very close to $C_{3v}$ in $(Ph_3P)_3AuCl$,[5] in the synthesis of anionic fullerene complexes. Previously, a series of molecular complexes of $\{(Ph_3P)AuCl\}_2\cdot C_{60}$, $\{(Ph_3P)AuCl\}_2\cdot C_{70}$, $\{(Anys_3P)AuCl\}_2\cdot C_{60}$, and $\{(Tol_3P)_2AuNO_3\}\cdot C_{60}$ compositions (Anys$_3$P: tri(*p*-anisyl)phosphine; Tol$_3$P: tri(*p*-tolyl)phosphine),[6] were synthesized using gold-containing compounds. Moreover, anionic fullerene complexes with gold-containing clusters, $\{(Ph_3P)_7Au_7^+\}_2\cdot(C_{60}^-)_2\cdot THF$ and $\{(Ph_3P)_7Au_8^{2+}\}_2\cdot(C_{60}^-)_2$,[7] are also known.

In this work, we report the layered anionic fullerene $C_{60}$ complex with gold $(Ph_3P)_3Au^+$ cations: $\{(Ph_3P)_3Au^+\}_2(C_{60}^{\bullet-})_2(C_{60})\cdot C_6H_4Cl_2$ (**1**). Indeed, the $C_{3v}$ symmetry of the cations allows the formation of hexagonal fullerene layers, in which the charge disproportionation among two monoanionic and one neutral fullerenes takes place. Such a phenomenon is very rare in fullerene complexes,[8] and we investigate possible reasons for the charge disproportionation. Crystal structure,

**Received:** March 24, 2014
**Published:** June 19, 2014

   dx.doi.org/10.1021/ic500689n | *Inorg. Chem.* 2014, 53, 6850−6855

optical, and magnetic properties of this complex are also discussed.

## RESULTS AND DISCUSSION

Crystals of $\{(Ph_3P)_3Au^+\}_2(C_{60}^{\bullet-})_2(C_{60})\cdot C_6H_4Cl_2$ (**1**) can be obtained with a poor yield through the reduction of an equimolar mixture of $C_{60}$ and $(Ph_3P)AuCl$ by a slight excess of sodium flourenone ketyl in *o*-dichlorobenzene. The $(Ph_3P)_3Au^+$ cations are formed most probably from three $(Ph_3P)AuCl$ molecules. Similarly, $\{(dppe)_2Co^+\}(C_{60}^{\bullet-})\cdot(C_6H_4Cl_2)_2$ was obtained by the reduction of a $C_{60}$ and $Co(dppe)Br_2$ mixture by TDAE, where dppe is 1,2-bis(diphenylphosphino)ethane.[9] Further, we modified the synthetic procedure and added 2 equiv of $Ph_3P$ prior to the reduction of the $C_{60}$-$(Ph_3P)AuCl$ mixture. In this case, the crystals of **1** were obtained with essentially higher yield and higher quality. The dark-brown plates of large size (up to $2 \times 2 \times 0.1$ mm$^3$) were obtained with 60% yield. The composition was determined from X-ray diffraction on single crystals. Several crystals tested from the synthesis had the same unit cell parameters, which showed the formation of one crystal phase only.

IR and UV−visible/NIR spectra of **1** are shown in the Supporting Information (Figures S2 and S3, respectively). The IR spectrum of **1** shows absorption bands of $(Ph_3P)_3Au^+$, fullerene $C_{60}$, and $C_6H_4Cl_2$ solvent molecules (Supporting Information, Table S1). There are two $(Ph_3P)_3Au^+$ cations per three fullerene molecules. The −2 charge can be distributed uniformly over three fullerenes with −0.67 electrons per on $C_{60}$, and in this case, salt **1** can be conducting. However, when charge disproportionation occurs, two electrons are localized on fullerenes to form two $C_{60}^{\bullet-}$ radical anions and leave one neutral $C_{60}$. Realization of the second possibility provides for charge localization and the absence of high conductivity. Optical spectra can answer the question on the charged state of fullerenes in **1** since the $F_{1u}(4)$ $C_{60}$ mode is sensitive to the charged state of the fullerene and is shifted from 1429 cm$^{-1}$ in the neutral state to 1396−1388 cm$^{-1}$ in the −1 charged state.[2e,10] An intermediate position between 1429 and 1396−1388 cm$^{-1}$ can originate from delocalization of electrons and an average −0.67 charge on fullerenes. The IR spectrum of **1** in the 1350−1450 cm$^{-1}$ range is shown in the Supporting Information (Figure S1). An intense broad band at 1392 cm$^{-1}$ corresponds to the formation of the $C_{60}^{\bullet-}$ radical anions. The band at 1434 cm$^{-1}$ is most probably due to the overlapping of two bands from neutral $C_{60}$ at 1429 cm$^{-1}$ and the band of starting $(Ph_3P)AuCl$ at 1434 cm$^{-1}$. That indicates the neutral state of fullerene since close positions of these bands are observed in the spectra of molecular complexes $\{(Ph_3P)AuCl\}_2\cdot C_{70}$ at 1433 cm$^{-1}$ and $\{(Ph_3P)AuCl\}_2\cdot C_{60}$ at 1436 and 1429 cm$^{-1}$. In any case, there are no absorption bands between 1434 and 1392 cm$^{-1}$ and partially charged fullerenes are absent in salt **1**, supporting the formation of negatively charged and neutral fullerenes. The UV−visible/NIR spectrum of **1** unambiguously indicates the formation of the $C_{60}^{\bullet-}$ radical anions due to the presence of characteristic absorption bands[10] at 1080 and 949 nm.

The crystal structure of **1** was determined for the crystal slowly cooled down to 100 K. Salt **1** has a highly symmetric trigonal lattice and contains one and a half crystallographically independent $C_{60}$ and one crystallographically independent $(Ph_3P)_3Au^+$ cation and $C_6H_4Cl_2$ solvent molecule. As a result, fullerenes and $C_6H_4Cl_2$ molecules located on the $C_{3v}$ symmetry axes are statistically disordered between three orientations (the $C_{3v}$ symmetry axis of the lattice does not coincide with the $C_{3v}$ symmetry axis of the $C_{60}$ molecule). This disorder cannot be suppressed by slower crystal cooling or the temperature decrease down to 90 K. Disorder of $C_{60}$ does not allow correct determination of the geometry of fullerenes in salt **1**. All figures in this report show only one orientation of three for the disordered components. The $(Ph_3P)_3Au^+$ cations are also located on the $C_{3v}$ symmetry axis of the lattice. However, since this axis coincides with the $C_{3v}$ symmetry axis of the $(Ph_3P)_3Au^+$ cation, they are ordered. The crystal structure shows a layered motif in which hexagonal fullerene layers alternate with the $\{(Ph_3P)_3Au^+\}_2(C_6H_4Cl_2)$ layers along the *c* axis (Figure 1). The most probable reason for why the simple

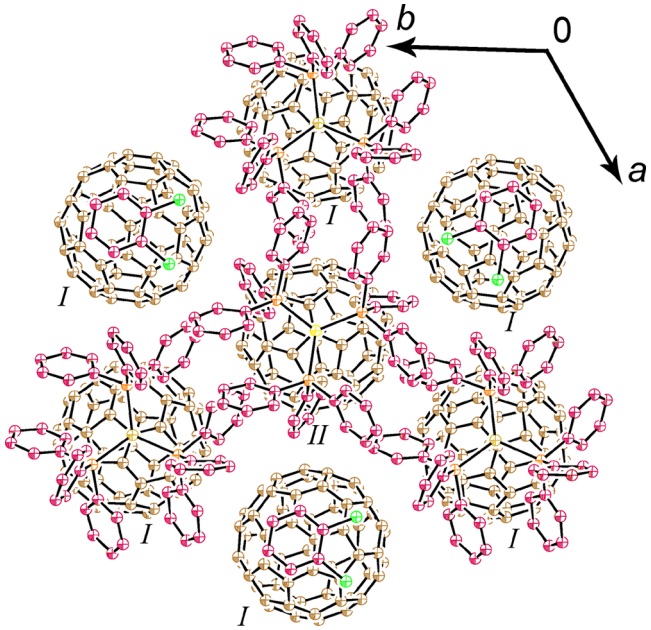


**Figure 1.** Projection of $\{(Ph_3P)_3Au^+\}_2\cdot C_6H_4Cl_2$ layers (carbon atoms are red-violet, chlorine atoms are green, phosphorus atoms are orange, and gold atoms are yellow) on hexagonal fullerene $C_{60}$ layers (carbon atoms are brown). View along the *c* axis is shown. Roman numerals show the type of fullerene: *I*, $C_{60}^{\bullet-}$; *II*, neutral $C_{60}$. Only one of three orientations is shown for $C_{60}$ and $C_6H_4Cl_2$ solvent molecules.

salt, $\{(Ph_3P)_3Au^+\}(C_{60}^{\bullet-})$, was not formed is that the $(Ph_3P)_3Au^+$ cations are too large to fit that of $C_{60}$, and one $(Ph_3P)_3Au^+$ cation is substituted by the $C_6H_4Cl_2$ solvent molecule, allowing the formation of closely packed hexagonal fullerene layers (see Figure 2). Since $(Ph_3P)_3Au^+$ and $C_6H_4Cl_2$ are distinctly different in size, interstitial sites are formed in the $\{(Ph_3P)_3Au^+\}_2(C_6H_4Cl_2)$ layer. To fill the vacancy, fullerenes move from the layers toward planar $C_6H_4Cl_2$ molecules. As a result, strongly corrugated fullerene layers are formed.

There are two types of fullerenes in **1** having different surroundings. Two of three fullerenes are denoted as type *I* in Figures 1−4. Each fullerene of type *I* is located close to one $(Ph_3P)_3Au^+$ cation and one $C_6H_4Cl_2$ molecule (Figure 3). In this case, positively charged gold cations approach close to the fullerenes, allowing the formation of a rather short $Au^+\cdots C(C_{60})$ distance of 4.80 Å. There are also several $H((Ph_3P)_3Au^+)\cdots C(C_{60})$ contacts shorter than the sum of van der Waals (vdW) radii between the cations and fullerenes, whereas $C_6H_4Cl_2$ solvent molecules do not form vdW C···C contacts with fullerenes (the contacts are longer than 3.54 Å). Since two


dx.doi.org/10.1021/ic500689n | Inorg. Chem. 2014, 53, 6850−6855

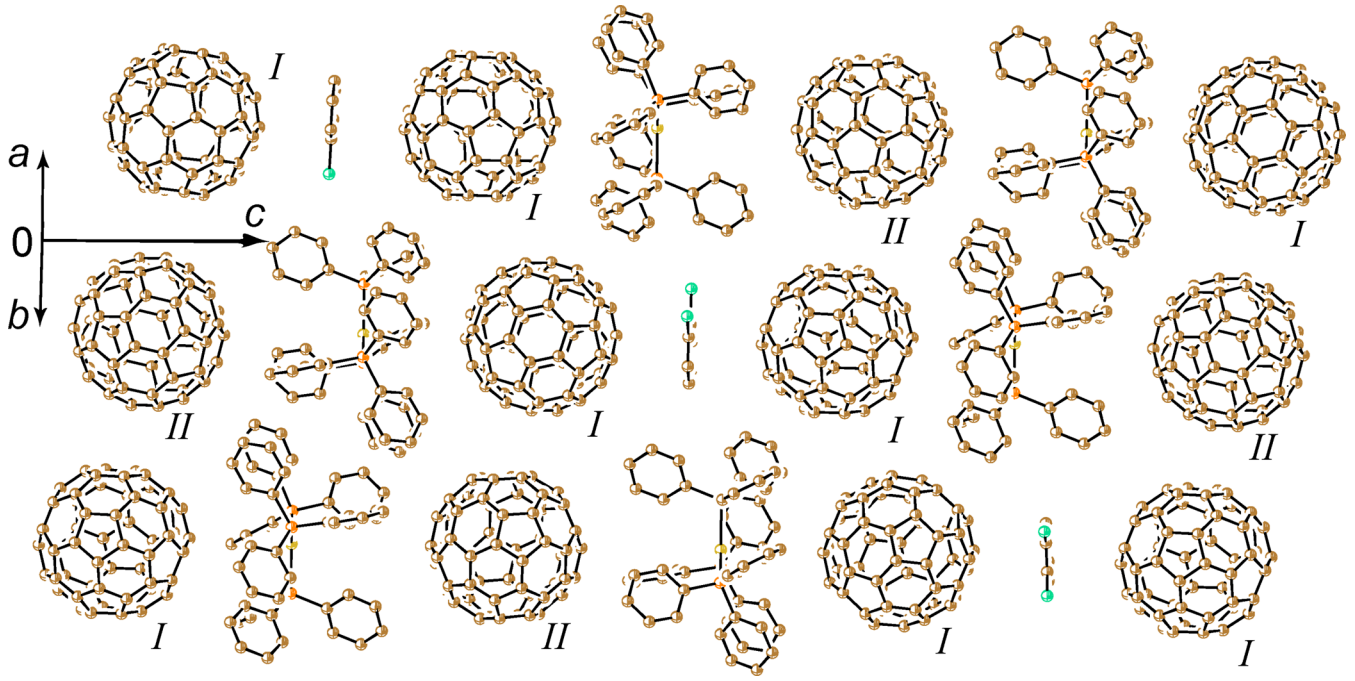


**Figure 2.** View along hexagonal fullerene layers and the diagonal of the *ab* plane. Roman numerals show the type of fullerene: *I*, $C_{60}^{\bullet-}$; *II*, neutral $C_{60}$. Only one of three orientations is shown for $C_{60}$ and $C_6H_4Cl_2$ solvent molecules.

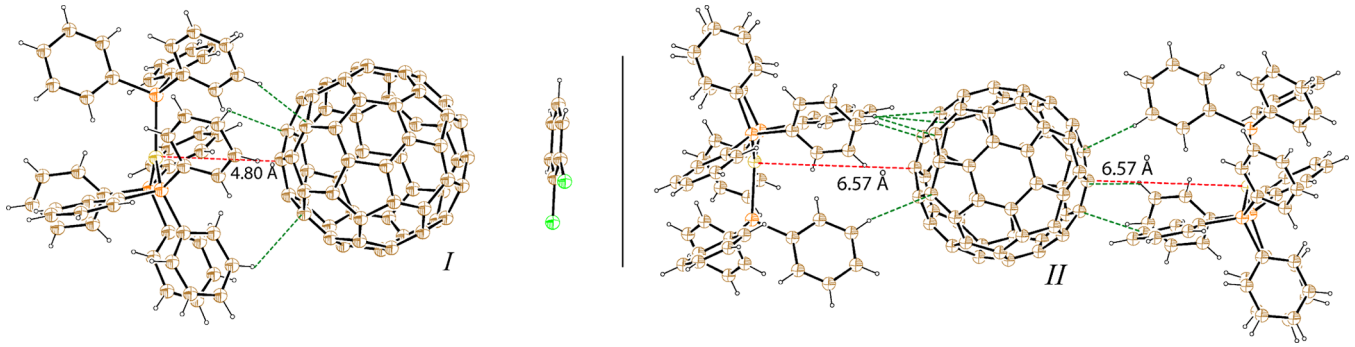


**Figure 3.** Cation and solvent surroundings for two types fullerenes: *I*, $C_{60}^{\bullet-}$ radical anions; *II*, neutral $C_{60}$. Short H, C({$Au^+(Ph_3P)_3$})···C($C_{60}$) contacts are shown by green dashed lines. The shortest Au···C($C_{60}$) contacts are shown by red dashed lines. Only one of three orientations is shown for $C_{60}$ and $C_6H_4Cl_2$ molecules.

of three fullerenes have such surroundings and the $Au^+$···C($C_{60}$) distances are shorter than that for another type of fullerene, we suppose a radical anion state for these fullerenes. One of three fullerenes is surrounded by two $(Ph_3P)_3Au^+$ cations (fullerenes of type *II* in Figures 1−4). The cations also form several short H($(Ph_3P)_3Au^+$)···C($C_{60}$) vdW contacts. However, the distances between positively charged gold atoms and fullerene carbons are 6.57 Å, i.e., essentially longer than those for fullerenes of type *I* (Figure 3). Since only one of three fullerenes of such type is present and it shows longer $Au^+$···C(fullerene) distances, we suppose a neutral state for these fullerenes. Charge disproportionation in the fullerene layers can be explained, namely, by different surroundings of fullerenes in **1**. The close location of positively charged $Au^+$ cations can localize negative charge on the fullerenes of type *I* due to the electrostatic stabilization between gold cations and fullerene anions. Charge disproportionation is rarely observed in ionic fullerene compounds.[8] In two previously described compounds, {(DMETEP$^+$)·$Zn^{II}$OEP}·($C_{60}^{\bullet-}$)·$(C_{60})_{0.5}$·$C_6H_4Cl_2$ (OEP is octaethylporphyrin; DMETEP$^+$ is *N*,*N*′-dimethyl-*N*′-ethylthioethylpiperazinium cation)[8a] and ($K^+$[DB18C6])$_4$-($C_{60}^{\bullet-}$)$_4$·($C_{60}$)·12THF (DB18C6 is dibenzo-18-crown-6 ether),[8b] negatively charged and neutral fullerenes have large spatial separation and in different cationic surroundings of fullerenes that easily provides charge disproportionation. The distances between two types of fullerenes are relatively short in **1**, and electrons can potentially move from charged to neutral fullerene. However, no movement is realized because of different cationic surroundings of negatively charged and neutral fullerenes.

Thus, hexagonal fullerene layers consist of negatively charged and neutral fullerenes (Figure 4). All center-to-center distances between differently charged fullerenes of types I and II are short (10.02 Å), and multiple short van der Waals (vdW) C···C contacts are formed between them, showing the formation of a closely packed fullerene structure. However, all center-to-center distances between negatively charged fullerenes of type I are essentially longer than those between type I and II fullerenes due to corrugation. The interfullerene center-to-center distances are 10.37 Å, and no vdW contacts form in this case.


dx.doi.org/10.1021/ic500689n | *Inorg. Chem.* 2014, 53, 6850−6855

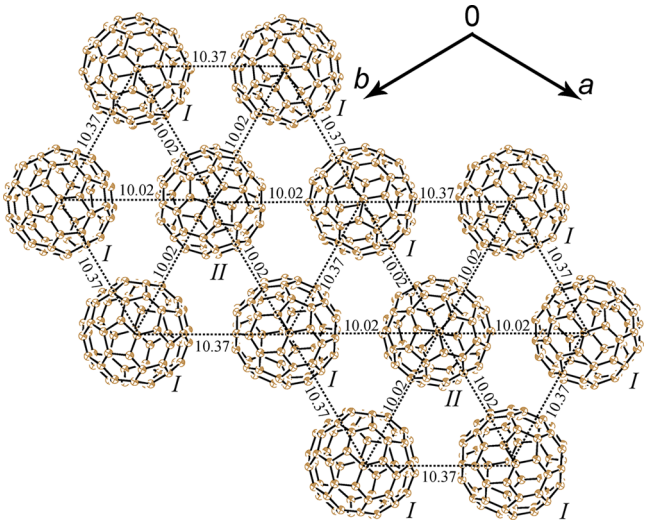


**Figure 4.** View on hexagonal fullerene layers and along the *c* axis. Roman numerals show the type of fullerene: *I*, $C_{60}^{\bullet-}$; *II*, neutral $C_{60}$. Black dashed lines linking fullerene centers and figures show interfullerene center-to-center distances in Angstroms. Only one of three orientations is shown for $C_{60}$.

That is possible since neighboring negatively charged fullerenes displace out of the layers toward $C_6H_4Cl_2$ in the opposite directions (above and below the fullerene layer). Neutral fullerenes of type II are completely surrounded by negatively charged fullerenes, and interfullerene center-to-center distances between them are longer than 17 Å. Thus, though hexagonal fullerene layers are formed with six fullerene neighbors for each fullerene, there are only three negatively charged fullerene neighbors for each $C_{60}^{\bullet-}$ located at interfullerene distances of 10.37 Å, essentially exceeding the vdW diameter of $C_{60}$ (10.18 Å).

The $\{(Ph_3P)_3Au^+\}$ cations have the $C_{3v}$ symmetry. As a result, all three P–Au bonds are equal to 2.3742(8) Å. The P–Au–P angles are equal to 120°, and the sum of these angles of 360° indicates a trigonal-planar arrangement. Thus, the purely ionic structure of the $(Ph_3P)_3Au^+$ cations is formed in the complex with $C_{60}$. The $Au^+$ cations slightly displace out of the plane formed by three phosphorus atoms by 0.005 and 0.010 Å toward closely located $C_{60}^{\bullet-}$ radical anions. Previously, solvent-free and dichloromethane-containing phases of $(Ph_3P)_3AuCl$ were structurally characterized. They do not show the $C_{3v}$ symmetry, and all three P–Au bonds are slightly different of 2.395(2), 2.404(2), and 2.432(2) Å for solvent-free and 2.3795(6), 2.3911(6), and 2.3666(6) Å for solvent-containing phases. The sum of three P–Au–P angles is 352.3° for the solvent-free phase and 355.35° for the solvent-containing phase, indicating a noticeable deviation of the $P_3Au$ core from planarity. This bonding situation is intermediate between covalent $[(Ph_3P)_3AuCl]$ and ionic $[(Ph_3P)_3Au^+](Cl^-)$ structures.

Magnetic properties of **1** were studied by EPR in the 297–4 K range (Figure 5). This compound showed an intense broad Lorentzian EPR signal with $g$ = 1.9984 and a line width ($\Delta H$) of 3.95 mT at 297 K (Figure 5a). This signal was unambiguously attributed[10,11] to $C_{60}^{\bullet-}$. Its integral intensity corresponds to the contribution of approximately two $S$ = 1/2 spins per formula unit, in accordance with the supposed ionic composition of **1**. The signal width strongly narrowed (Supporting Information, Figure S4), and the $g$-factor was shifted to smaller values with cooling (Figure 5c). The temperature dependence of the reverse integral intensity of the signal can be fitted well by the Curie–Weiss law with a negative Weiss temperature of −5 K (Figure 5d), showing weak antiferromagnetic interaction of spins. Most probably, this interaction results in the splitting of the EPR signal into two components below 75 K (Figure 5b), which also narrow and shift to the smaller $g$-factors with the temperature decrease (Figure S4, Supporting Information, and Figure 5c). The weakness of the antiferromagnetic interaction can be interpreted by poor numbers (only three) of negatively charged fullerene neighbors with long distances.

The electrical resistance of single crystals of **1** was measured by a two-probe technique along the fullerene plane in anaerobic conditions. The contacts are fixed on a single crystal with carbon paste (JEOL Dotite). The crystal has a resistance of ca. $3\cdot10^8$ Ω (ca. $4\cdot10^5$ Ω·cm in the electrical resistivity), supporting the highly resistive state of compound **1**.

The new fullerene $C_{60}$ salt with gold cations, $\{(Ph_3P)_3Au^+\}_2(C_{60}^{\bullet-})_2(C_{60})\cdot C_6H_4Cl_2$ (**1**), was obtained. Cations have the $C_{3v}$ symmetry, providing the formation of hexagonal

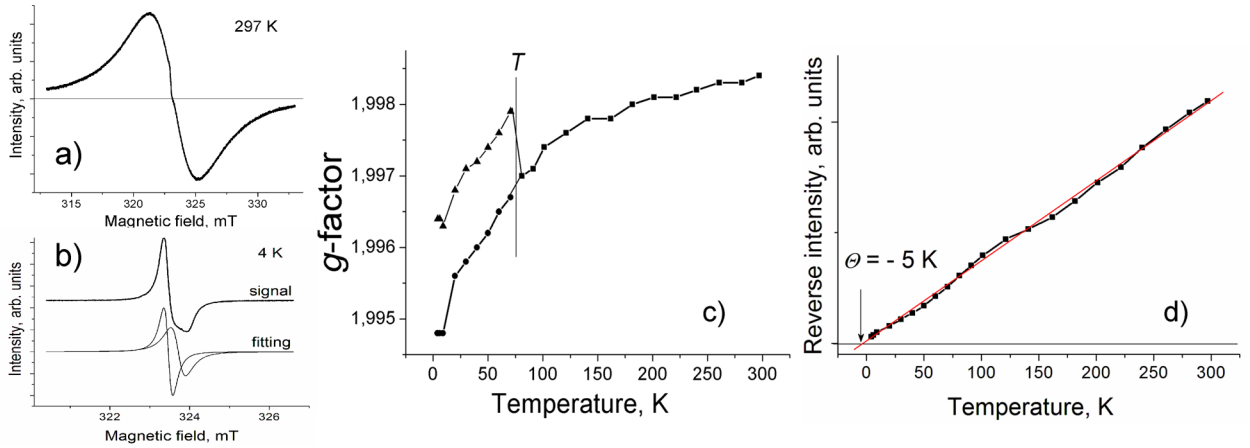


**Figure 5.** EPR signal of **1** attributed to $C_{60}^{\bullet-}$ at (a) 297 and (b) 4 K. The fitting of the EPR signal by two Lorentzian lines is shown below the experimental curve. (c) Temperature dependence of $g$-factor of the EPR signal from polycrystalline **1**. *T* marks temperature of the EPR signal splitting into two lines. (d) Temperature dependence of reverse integral intensity fitted by the Curie–Weiss law with a Weiss temperature of −5 K (red line).


dx.doi.org/10.1021/ic500689n | *Inorg. Chem.* 2014, 53, 6850–6855

fullerene layers. There are two gold cations per three fullerene molecules. However, the negative charge is distributed nonuniformly over fullerene layers. Charge disproportionation is accompanied by the formation of negatively charged and neutral fullerenes of types *I* and *II*, respectively. These fullerenes have different cationic surroundings and distances to $Au^+$. Most probably, the closer location of $Au^+$ to fullerenes of type *I* results in the localization of negative charge on these fullerenes. Such charge disproportionation in hexagonal fullerene layers is observed for the first time since, in previously studied compounds with charge disproportionation, negatively charged and neutral fullerenes had large spatial separation. Charged and neutral fullerenes in **1** are closely packed within the layers, and the distances between $C_{60}^{\bullet-}$ are noticeably longer due to corrugation of the layers. Thus, in spite of hexagonal packing and close arrangement of fullerenes in the layers, high conductivity is not realized in the salt due to charge disproportionation. The degree of magnetic interactions of spins in the fullerene layers is not high due to relatively long distances between negatively charged fullerenes. Nevertheless, structural modification of salt **1** by gold cations with the $C_{3v}$ symmetry and smaller size can afford salts with more uniform hexagonal fullerene layers and full charge transfer to fullerenes like in $(MDABCO^+)(C_{60}^{\bullet-})(TPC)$ metal. This work is now in progress.

## EXPERIMENTAL SECTION

**Materials.** $(Ph_3P)AuCl$ (99.9%) and $Ph_3P$ (99%) were purchased from Aldrich. Sodium fluorenone ketyl used for fullerene reduction was obtained as previously described.[12] $C_{60}$ of 99.98% purity was purchased from MTR Ltd. All manipulations for the synthesis of **1** were carried out in a MBraun 150B-G glovebox with a controlled inert atmosphere, and the contents of $H_2O$ and $O_2$ were less than 1 ppm. Solvents were purified in an argon atmosphere. *o*-Dichlorobenzene ($C_6H_4Cl_2$) was distilled over $CaH_2$ under reduced pressure, and hexane was distilled over Na/benzophenone. The crystals of **1** were stored in the glovebox. KBr pellets for the measurements of IR and UV−visible/NIR spectra were also prepared in a glovebox. EPR measurements were performed on the collection of single crystals of **1** sealed in 2 mm quartz tubes.

**Synthesis.** Preliminary synthesis of $\{(Ph_3P)_3Au^+\}_2(C_{60}^{\bullet-})_2(C_{60})\cdot C_6H_4Cl_2$ (**1**) was carried out by the following procedure. Fullerene $C_{60}$ (30 mg, 0.042 mmol), a stoichiometric amount of $(Ph_3P)AuCl$ (21 mg, 0.042 mmol), and slight excess of sodium fluorenone ketyl (10 mg, 0.049 mmol) in 14 mL of *o*-dichlorobenzene were stirred at 80 °C during 2 h. The color of the solution turned red violet, and the NIR spectrum of the solution showed the formation of the $C_{60}^{\bullet-}$ radical anions. The cooled solution was filtered in a 50 mL glass tube of 1.8 cm in diameter with a ground glass plug, and 30 mL of hexane was layered over the obtained solution. The crystals of the salt precipitated during 1 month as dark brown plates. The solvent was decanted from the crystals, and they were washed with hexane. Crystals with the size up to 0.5 × 0.5 × 0.1 $mm^3$ were obtained with 24% yield.

An improved synthesis of **1** was performed by adding 2 equiv of $Ph_3P$ (22 mg, 0.084 mmol) to the solution of $(Ph_3P)AuCl$ (21 mg, 0.042 mmol) in 14 mL of *o*-dichlorobenzene, and the solution was stirred at 80 °C during 2 h, leaving a colorless solution. After $C_{60}$ (30 mg, 0.042 mmol) and a slight excess of sodium fluorenone ketyl (10 mg, 0.049 mmol) were added, the synthesis of crystals was carried out similarly to the above method. The crystals of the complex were precipitated during 1 month as large dark-brown plates (up to 2 × 2 × 0.1 $mm^3$). The solvent was decanted from the crystals, and they were washed with hexane. The crystals were obtained with 60% yield. IR and UV−visible spectra and unit cell parameters of the salts obtained by both methods are the same, showing that only one crystal phase is formed in both syntheses.

The composition of **1** was determined from X-ray diffraction on single crystals. Several crystals tested from the synthesis had the same unit cell parameters.

**General.** UV−visible/NIR spectra were measured in KBr pellets on a PerkinElmer Lambda 1050 spectrometer in the 250−2500 nm range. FT-IR spectra were obtained in KBr pellets with a PerkinElmer Spectrum 400 spectrometer (400−7800 $cm^{-1}$). EPR spectra were recorded for a polycrystalline sample of **1** from 4 K up to 297 K with a JEOL JES-TE 200 X-band ESR spectrometer equipped with a JEOL ES-CT470 cryostat. For the estimation of a number of spins in **1**, the integral intensity of the signal from a weighed amount of the complex was compared with that of the signal from a sample of $CuSO_4\cdot 5H_20$ with a known number of spins.

**X-ray Crystallographic Study.** Crystal data for **1** at 100(2) K: $C_{147}H_{47}AuClP_3$, $M_r$ = 2138.17, brown plate, trigonal, $R\bar{3}c$ (No. 167), $a$ = 17.1760(6) Å, $b$ = 17.1760(4) Å, $c$ = 101.643(11) Å, $V$ = 25969(3) $Å^3$, $Z$ = 12, $d_{calc}$ = 1.641 $g\cdot cm^{-3}$, $\mu$ = 1.854 $mm^{-1}$, $F(000)$ = 12 840, $2\theta_{max}$ = 58.653°, reflections measured 76 013, unique reflections 7629, reflections with $I > 2\sigma(I)$ = 5367, parameters refined 867, restraints 8317, $R_1$ = 0.0379, $wR_2$ = 0.1025, G.O.F. = 1.035, CCDC 993197.

X-ray diffraction data for **1** were collected at 100(2) K on a Bruker Smart Apex II CCD diffractometer with graphite monochromated Mo K$\alpha$ radiation using a Japan Thermal Engineering Co. cooling system DX-CS190LD. Raw data reduction to $F^2$ was carried out using Bruker SAINT.[13] The structures were solved by the direct method and refined by the full-matrix least-squares method against $F^2$ using SHELX-2013.[14] Non-hydrogen atoms were refined in the anisotropic approximation. Positions of hydrogen atoms were included into refinement in a riding mode.

The crystal structure of **1** at 100(2) K contains two crystallographically independent $(Ph_3P)_3Au^+$ cations, three fullerenes, and one $C_6H_4Cl_2$ solvent molecule. Fullerenes and the $C_6H_4Cl_2$ molecule are located on the $C_{3v}$ symmetry axes and are statistically disordered between three orientations. To keep the fullerene geometry close to the ideal one in the disordered groups, the bond length restraints were applied along with the next-neighbor distances, using the SADI SHELXL instruction. That results in a great number of restraints used for the refinement of the crystal structure of **1**.

## ASSOCIATED CONTENT

### Supporting Information

Table of IR spectra data; figures showing IR spectra, UV−visible/NR spectrum, and temperature dependence of the line width of the EPR signal; and crystallographic data in CIF format. This material is available free of charge via the Internet at http://pubs.acs.org.

## AUTHOR INFORMATION

### Corresponding Author

*Fax: +007-496-522-18-52. E-mail: konarev@icp.ac.ru.

### Notes

The authors declare no competing financial interest.

## ACKNOWLEDGMENTS

The work was supported by the Russian Science Foundation (project N 14-13-00028) and Grant-in-Aid Scientific Research from JSPS, Japan (23225005), and MEXT, Japan (20110006).

## REFERENCES

(1) (a) Allemand, P.-M.; Khemani, K. C.; Koch, A.; Wudl, F.; Holczer, K.; Donovan, S.; Grüner, G.; Thompson, J. D. *Science* **1991**, *253*, 301. (b) Narimbetov, B.; Omerzu, A.; Kabanov, V. V.; Tokumoto, M.; Kobayashi, H.; Mihailovic, D. *Nature* **2000**, *407*, 883.

(2) (a) Kobayashi, H.; Tomita, H.; Moriyama, H.; Kobayashi, A.; Watanabe, T. *J. Am. Chem. Soc.* **1994**, *116*, 3153. (b) Moriyama, H.; Kobayashi, H.; Kobayashi, A.; Watanabe, T. *Chem. Phys. Lett.* **1995**, *238*, 116. (c) Douthwaite, R. E.; Green, M. A.; Green, M. L. H.;

Rosseinsky, M. J. *J. Mater. Chem.* **1996**, *6*, 1913. (d) Konarev, D. V.; Khasanov, S. S.; Otsuka, A.; Maesato, M.; Saito, G.; Lyubovskaya, R. N. *Angew. Chem., Int. Ed.* **2010**, *49*, 4829. (e) Konarev, D. V.; Lyubovskaya, R. N. *Russ. Chem. Rev.* **2012**, *81*, 336.
(3) (a) Hönnerscheid, A.; Wüllen, L.; Jansen, M.; Rahmer, J.; Mehring, M. *J. Chem. Phys.* **2001**, *115*, 7161. (b) Konarev, D. V.; Khasanov, S. S.; Otsuka, A.; Saito, G. *J. Am. Chem. Soc.* **2002**, *124*, 8520. (c) Konarev, D. V.; Khasanov, S. S.; Saito, G.; Otsuka, A.; Yoshida, Y.; Lyubovskaya, R. N. *J. Am. Chem. Soc.* **2003**, *125*, 10074. (d) Domrachev, G. A.; Shevelev, Yu. A.; Cherkasov, V. K.; Markin, G. V.; Fukin, G. K.; Khorshev, S. Ya.; Kaverin, B. S.; Karnatchevich, V. L. *Russ. Chem. Bull.* **2004**, *53*, 2056. (e) Konarev, D. V.; Khasanov, S. S.; Kovalevsky, A. Y.; Saito, G.; Otsuka, A.; Lyubovskaya, R. N. *Dalton Trans.* **2006**, 3716. (f) Konarev, D. V.; Khasanov, S. S.; Saito, G.; Otsuka, A.; Lyubovskaya, R. N. *J. Mater. Chem.* **2007**, *17*, 4171. (g) Konarev, D. V.; Khasanov, S. S.; Lyubovskaya, R. N. *Russ. Chem. Bull.* **2007**, *56*, 371.
(4) Konarev, D. V.; Khasanov, S. S.; Otsuka, A.; Maesato, M.; Uruichi, M.; Yakushi, K.; Shevchun, A.; Yamochi, H.; Saito, G.; Lyubovskaya, R. N. *Chem. - Eur. J.* **2014**, *20*, 7268.
(5) (a) Hamel, A.; Schier, A.; Schmidbaur, H. *Z. Naturforsch.* **2002**, *57b*, 877. (b) Jones, P. G.; Sheldrick, G. M.; Muir, J. A.; Muir, M. M.; Pulgar, L. B. *J. Chem. Soc., Dalton Trans.* **1982**, 2123.
(6) (a) Balch, A. L.; Olmstead, M. M. *Coord. Chem. Rev.* **1999**, *185*−*186*, 601. (b) Graja, A.; Waplak, S.; Gritsenko, V. V.; Spitsina, N. G.; Drichko, N. V. *Synth. Met.* **1999**, *106*, 29. (c) Graja, A.; Lipiec, R.; Waplak, S.; Krol, S.; Turowska-Tyrk, I.; Drichko, N. V. *Chem. Phys. Lett.* **1999**, *313*, 725. (d) Schulz-Dobrick, M.; Jansen, M. *CrystEngComm* **2008**, *10*, 661. (e) Schulz-Dobrick, M.; Jansen, M. *Z. Anorg. Allg. Chem.* **2008**, *634*, 817.
(7) Schulz-Dobrick, M.; Jansen, M. *Angew. Chem., Int. Ed.* **2008**, *47*, 2256.
(8) (a) Konarev, D. V.; Khasanov, S. S.; Saito, G.; Lyubovskaya, R. N. *Cryst. Growth Des.* **2009**, *9*, 1170. (b) Kozhemyakina, N. V.; Amsharov, K. Yu.; Nuss, J.; Jansen, M. *Chem. - Eur. J.* **2011**, *17*, 1798.
(9) Konarev, D. V.; Kuzmin, A. V.; Simonov, S. V.; Khasanov, S. S.; Yudanova, E. I.; Lyubovskaya, R. N. *Dalton Trans* **2011**, *40*, 4453.
(10) (a) Reed, C. A.; Bolskar, R. D. *Chem. Rev.* **2000**, *100*, 1075. (b) Konarev, D. V.; Lyubovskaya, R. N. *Usp. Khim.* **1999**, *68*, 19.
(11) (a) Allemand, P. M.; Spdanov, G.; Koch, A.; Khemani, K.; Wudl, F.; Rubin, Y.; Diederich, F.; Alvarez, M. M.; Anz, S. J.; Whetten, R. L. *J. Am. Chem. Soc.* **1991**, *113*, 2780. (b) Konarev, D. V.; Kovalevsky, A.Yu.; Khasanov, S. S.; Saito, G.; Otsuka, A.; Lyubovskaya, R. N. *Eur. J. Inorg. Chem.* **2005**, 4822.
(12) Konarev, D. V.; Khasanov, S. S.; Yudanova, E. I.; Lyubovskaya, R. N. *Eur. J. Inorg. Chem.* **2011**, 816.
(13) *SAINT*; Bruker Analytical X-ray Systems: Madison, WI, 1999.
(14) Sheldrick, G. M. *SHELXL2013*; University of Göttingen: Göttingen, Germany, 2013.


dx.doi.org/10.1021/ic500689n | *Inorg. Chem.* 2014, 53, 6850−6855